TECHNO-ECONOMIC ANALYSIS OF THE SUB-CRITICAL ORC WITH OPTIMIZED HEAT TRANSFER PROCESS

Wei Liu[1,*], Dominik Meinel[1], Christoph Wieland[1] and Hartmut Spliethoff[1,2]

[1]Institute for Energy Systems, Faculty of Mechanical Engineering, Technische Universität München
Boltzmannstrasse 15, 85748
Garching, Germany

[2]The Bavarian Center for Applied Energy Research (ZAE Bayern), Division 1: Technology for Energy Systems and Renewable Energy, Walther-Meissner-Str. 6, 85748
Garching, Germany
wei.liu@tum.de

* Corresponding Author

ABSTRACT

A techno-economic analysis of a sub-critical ORC designed for the utilization of geothermal heat is performed. The thermodynamic optimization of the investigated ORC system is based on a new approach, in which thermal match between the heat source and the working fluid is improved by operating an optimal working fluid at near-critical pressures. The Optimal Heat Source Temperature (OHST) method is used to identify suitable fluids for which the pinch point is located at the inlet (or an intermediate point) of the preheater. As a result, R227ea is selected, which performs best under certain defined conditions, while R245fa is also considered as a reference fluid for further thermo-economic comparison. A heat transfer model is proposed for the plate heat exchanger system in order to determine the pinch point position in the case of near-critical fluid parameters, as well as to obtain the heat transfer area which is required for the calculation of Purchased Equipment Cost (PEC). The economic optimization is based on the minimization of the Levelized Cost of Electricity (LCOE) for the considered fluids. Results from the techno-economic optimizations show that for R245fa the optimum is obtained with a system efficiency of 7.306% and a LCOE of 205.7 €/MWh. In comparison, the proposed approach for R227ea leads to an optimum with a system efficiency of 8.607% and a LCOE of 185.9 €/MWh. The comparison suggests that although the proposed approach aims to improve the thermodynamic performance of the sub-critical ORC, it is also promising in terms of the economic profitability.

1. INTRODUCTION

Interests on power generation from low temperature geothermal heat have grown rapidly in the past decades due to the increase in the electricity consumption worldwide. The Organic Rankine Cycle (ORC) system has been considered as one of the most suitable technologies for the exploitation of such heat source because of several advantages, such as simplicity and relatively high efficiency compared to the conventional water/steam Rankine cycle. However, a great limitation of improving the system efficiency of ORC is the isothermal evaporation which leads to a high exergy destruction in the heat transfer process. Several methods are available, aiming at a better thermal match between the heat source and the working fluid, such as using triangular ORC (Khennich and Galanis, 2012) or super-critical ORC to bypass the isothermal evaporation (Schuster *et al*., 2010), or using fluid mixtures in order to obtain a non-isothermal evaporation (Heberle *et al*., 2012). Although these techniques are effective under certain working conditions, the complexity of the ORC system or of the component is increased, causing higher manufacturing costs.

To reduce the exergy destruction caused by isothermal evaporation, an interesting approach is proposed in this paper, where a very high evaporation temperature is applied in order to reduce the absolute heat amount transferred during the evaporation process. The drawback of this approach is, however, obvious: the pinch point which is in most cases located at the evaporator inlet can greatly

limit the mass flow rate of the working fluid, leading to a reduced power output. To overcome this drawback, it is prerequisite for the proposed approach to find a suitable working fluid, for which the pinch point is located not at the evaporator inlet but the preheater inlet. As a result, the whole heat transfer process is optimized, leading to a better thermal match and hence a higher system efficiency (Liu *et al.*, 2014, 2015).

Although the proposed approach has been proven to be an effective method for improving the thermodynamic performance, its impact on the economic performance is still uncertain: the better thermal match in the preheating process does lead to a higher system performance; however, it requires a larger heat transfer area, which increases the purchase cost of the heat exchanger system. Therefore, the main task of the present paper is the thermo-economic investigation of the ORC which is optimized using the proposed approach for the geothermal power generation.

2. Modeling and Thermodynamic Description of Subcritical ORC

Figure 1(a) shows the considered subcritical ORC, which includes the most fundamental components: pump, preheater, evaporator, turbine and condenser. The working fluid at the saturated liquid state (state 1) is pressurized in the pump to a high pressure (state 2). Then it is led to the preheater where the sub-cooled fluid is heated until being liquidly saturated (state 3). Afterwards, the saturated liquid is evaporated under isothermal condition to the saturated vapor (state 4). The vapor then expands in the turbine, which rotates the shaft and generates electricity. At last, the loop is closed by condensing the super-heated vapor (state 5) to the saturated liquid (state 1).
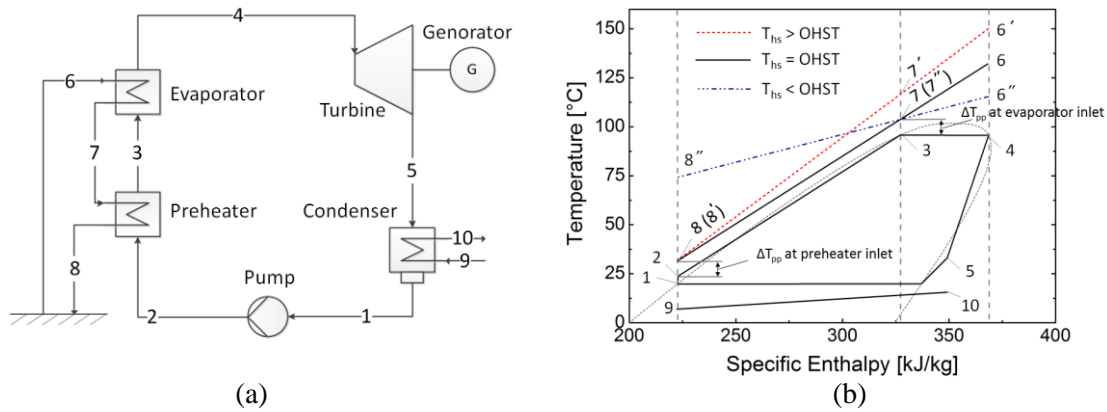

Figure 1: (a) Schematic diagram of a standard ORC, (b) Demonstration of OHST in T-h diagram

The static cycle simulation is performed in Matlab, using fluid properties from REFPROP 9.0 (Lemmon *et al.*, 2012). Simplifications are made that (1) there is no heat loss and no pressure drop through the cycle; (2) auxiliary power consumption, e.g. power required for circulating pump is neglected. The balance strategy is to vary the mass flow rate for the working fluid and the cooling water until the pinch point meets the design criteria in the heat exchanger and condenser, respectively. Unlike the common cycle simulations, the pinch point in the heat exchanger is considered as variable. Table 1 summarizes all boundary conditions for the cycle simulation.

Table 1: Boundary conditions for the investigated subcritical ORC.

Heat source temperature	T_{hs}	140 °C	Cooling water temperature	T_{cw}	8 °C
Heat source pressure	p_{hs}	10 bar	Cooling water pressure	p_{cw}	1 bar
Heat source thermal amount	$\dot{Q}_{hs}$	50 MW	Isentropic efficiency Turbine	$\eta_{is,turbine}$	0.85
Evaporating pressure	p_{evp}	< 30 bar	Isentropic efficiency Pump	$\eta_{is,pump}$	0.75
Pinch point in heat exchanger	$\Delta T_{pp,HE}$	Variable	Mechanical efficiency	η_{mech}	0.98
Condensation temperature	T_{cond}	20 °C	Generator/Motor efficiency	η_G/η_M	0.95
Pinch point in the condenser	ΔT_{cond}	5 K	Reference state	p_0, T_0	1 bar, 8 °C

Global system efficiency which combines both thermal efficiency η_{th} and heat transfer efficiency η_{HT} of the ORC system is used in this study for the evaluation of the thermodynamic performance. It is given by (Schuster *et al.*, 2010):

$$\eta_{sys} = \eta_{th} \cdot \eta_{HT} \qquad (1)$$

Where η_{th} and η_{HT} are equal to:

$$\eta_{th} = \frac{P_{el,net}}{\dot{Q}_{HT}} = \frac{\eta_{mech} \cdot \eta_G \cdot (h_4 - h_5) - (h_2 - h_1)/\eta_{mech}/\eta_M}{h_4 - h_2} \qquad (2)$$

$$\eta_{HT} = \frac{\dot{Q}_{HT}}{\dot{Q}_{hs}} = \frac{h_6 - h_8}{h_6 - h_0} \qquad (3)$$

Where $P_{el,net}$ is the net power output [kW]; $\dot{Q}_{HT}$ is the heat flow transferred from the heat source to the ORC unit [kW]; $\dot{Q}_{hs}$ represents the available heat of the considered heat source [kW].

Therefore, to increase the thermal efficiency η_{th} of the investigated ORC system with a constant condensation temperature it is practical to increase the evaporating pressure p_4. To increase the heat transfer efficiency η_{HT}, the heat source outlet temperature T_8 should be lowered as much as possible. More specifically, the maximum of η_{HT} can be observed when the pinch point is located at the preheater inlet.

3. Optimal Heat Source Temperature

The Optimal Heat Source Temperature (OHST) is defined as a heat source temperature, for which the pinch point is evenly located in the preheater (Liu *et al*. 2015). By comparing the OHST with the available heat source temperature, the pinch point position for the investigated ORC can be identified, which is demonstrated by figure 1(b). In the case where $T_{hs} <$ OHST, the pinch point is located at the evaporator inlet (states 3-7(7″)). In the case where $T_{hs} >$ OHST, however, the pinch point is shifted to the preheater inlet (states 2-8(8')). As the proposed approach requires a pinch point position at the preheater inlet, the working fluid selection should be based on a condition that the OHST is lower than the available heat source temperature.

Assuming a constant specific heat capacity for the homogeneous liquid, the OHST can be estimated as a state quantity depending only on the evaporating pressure (Liu *et al*., 2015), provided that the pinch point and the condensation temperature are constant:

$$OHST = \frac{h_{evp}}{\bar{c}_{p,wf}} + T_{evp} + \Delta T_{pp,evp} \qquad (4)$$

Where the mean specific heat capacity for the working fluid is calculated by:

$$\bar{c}_p = \frac{h_3 - h_2}{T_3 - T_2} \qquad (5)$$

Where T_2 is assumed equal to the condensation temperature of the working fluid, since temperature changes only slightly for a homogenous liquid after compression.

The fluid screening is performed based on the OHST theory mentioned above. Firstly, 35 pure fluids with the critical temperatures between 90 and 160 °C are selected out of 121 fluids from the REFPROP database. Afterwards, the OHSTs are calculated for all the considered fluids using equation (4) and (5) given a constant pinch point of 10 K and the evaporating pressure of $0.9 \cdot p_c$, which are summarized in figure 2. It is noted that the constant pinch point is considered in this section only for the purpose of the screening of fluids. Next, taking into account the boundary conditions that $p_{evp} < 30$ bar and OHST $< T_{hs}$ (140 °C), the only fluid, i.e. R227ea which is located near the bottom left corner of figure 2 can be selected for the further cycle simulations. In addition, R245fa which has been widely used in the ORC industry is also selected as a reference fluid for comparison.

It should be noted that in the case of near-critical fluid parameters the pinch point can be located neither in the preheater inlet nor the evaporator inlet, since the heat capacity is strongly dependent on

the temperature. Figure 3(a) presents a possible scenario where the pinch point is located at an intermediate point of the preheater. In order to predict such pinch point position, it is necessary to partition the preheating process into finite number of elements assuming an equal amount of transferred heat, which is detailed in section 4.
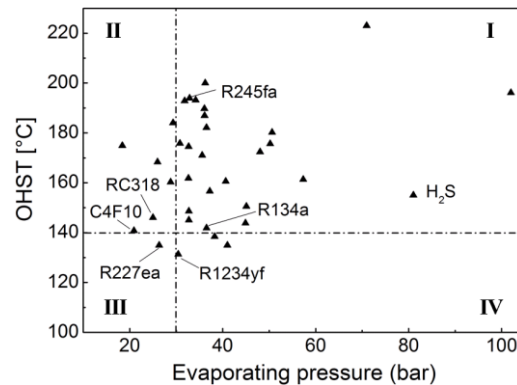

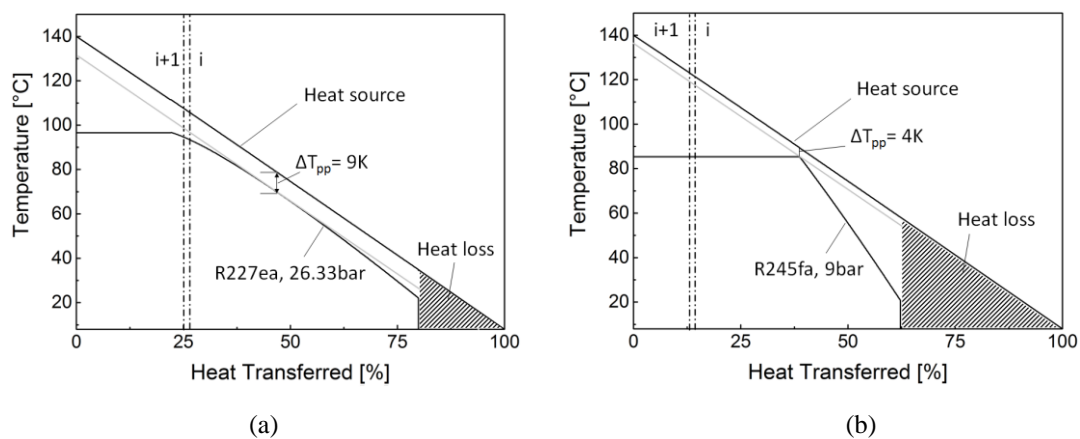**Figure 2:** OHST versus evaporating pressure for the considered fluids.

| (a) | (b) |

Figure 3: Demonstration of TQ-diagram and pinch point position for (a) R227ea and (b) R245fa, respectively.

4. Heat Transfer calculation

The main aims of the heat transfer calculations are 1) the determination of the pinch point location demonstrated similar to figure 3, and 2) the calculation of the heat transfer coefficient and the required surface area for a counter-flow plate heat exchanger system. The preheater and evaporator are considered as a whole in order to simplify the system components. Assumptions are made that the heat transfer process is stationary and both of the pressure drop and the fouling factor are negligible.

Based on the given geometric parameters of the plate (see table 2), the sizing of a Plate Heat Exchanger (PHE) system requires only few characteristics, i.e. plate arrangement, plates (channel) number and the channel spacing. Figure 4 demonstrates the plate arrangement of the considered PHE system, where plates are arranged into three blocks to form equal number of parallel channels. The channel spacing is set to 3.6 mm. The channel number for each fluid is related to the total required surface area.

Taking into account the temperature dependency of heat capacity, the assumption of an overall temperature difference between the hot and cold fluids cannot be acceptable for the investigated preheating process. For this reason, both of the preheating and evaporating processes are discretized respectively into a number of elements with equal amount of heat flow, as demonstrated in figure 3 and 4. For reduction of the calculation error, the number of elements N_{ele} is set to 500 (Karellas *et al*. 2012).

Table 2: Input parameters for plate.

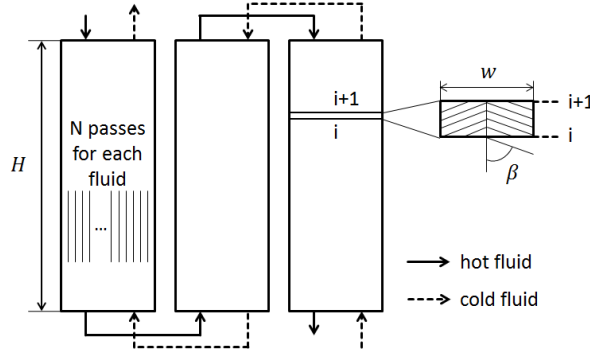|		
Plate width	W	0.7 m
Plate height	H	2.31 m
Channel space	b	3.6 mm
Corrugation angle	β	60°
Plate thickness	d_{plate}	0.7 mm
Thermal conductivity	λ_{plate}	15 W/m·K

Figure 4: Schematic overview of the plate heat exchanger system.

Within each element, the transferred amount of heat flow is thus given by:

$$\dot{Q}_i = \frac{\dot{Q}_{HT}}{N_{ele}} = U_i \cdot A_i \cdot \Delta T_i \tag{6}$$

$$= \dot{m}_{hs,i} \cdot c_{p,hs,i} \cdot \left(T_{hs,i+1} - T_{hs,i}\right) = \dot{m}_{wf,i} \cdot c_{p,wf,i} \cdot \left(T_{wf,i+1} - T_{wf,i}\right)$$

Where $\dot{m}_i$ is equal to $\dot{m}/N_{ch}$ [kg/s]; and ΔT_i is simplified for each element by assuming:

$$\Delta T_i = T_{hs,i} - T_{wf,i} \tag{7}$$

On this account, the pinch point can be obtained by:

$$\Delta T_{pp} = \min_{1 \leq i \leq N_{ele}} \Delta T_i \tag{8}$$

Assuming the convective heat transfer is dominant, the overall heat transfer coefficient is given by:

$$\frac{1}{U_i} = \frac{1}{h_{wf,i}} + \frac{d_{plate}}{\lambda_{plate}} + \frac{1}{h_{hs,i}} \tag{9}$$

To calculate the convective heat transfer coefficient at an arbitrary point i, it is necessary to obtain the Nusselt number which is defined as the ratio of convective to conductive heat transfer across the elementary boundary:

$$Nu_i = \frac{h_i \cdot D_h}{\lambda_i} \rightarrow h_i = \frac{Nu_i \cdot \lambda_i}{D_h} \tag{10}$$

Where λ_i is the thermal conductivity at point i [W/m^{2}K]; D_h [m] is the hydraulic diameter which is equal to $2Wb/(W + b)$ referring to the investigated plate channel.

Depending on the type of the heat transfer process, the Nusselt numbers are calculated using various empiric correlations. For the single-phase heat transfer process, the Chisholm and Wanniarachchi (Chisholm and Wanniarachchi, 1990) correlation is employed where Nusselt number is given by:

$$Nu = 0.724 \cdot \left(\frac{6\beta}{\pi}\right)^{0.646} \cdot Re^{0.583} \cdot Pr^{0.33} \tag{11}$$

Where Pr is the dimensionless Prandtl number, given by $Pr = c_p \cdot \mu/\lambda$.

For the multi-phase heat transfer, the working fluid undergoes the liquid-gaseous phase transition. Specifically for the evaporating process, Nusselt number is calculated using Yan and Lin's correlation (Yan and Lin, 1999):

$$Nu = 1.926 \cdot Pr_l^{0.33} \cdot Bo_{eq}^{0.3} \cdot Re_{eq}^{0.5} \left[(1-x) + x \cdot \left(\frac{\rho_l}{\rho_v} \right)^{0.5} \right] \tag{12}$$

Where Bo_{eq} is the equivalent boiling number; Re_{eq} is the equivalent Reynold number; ρ_l is the density for saturated liquid [kg/m³]; ρ_v is the density for saturated vapor [kg/m³]; x is vapor fraction. It should be noted that for obtaining the continuous heat transfer coefficient the Nusselt number for the evaporative heat transfer is modified by multiplying equation (12) by a factor X_{Nu} given by:

$$X_{Nu} = \frac{Nu_{pre,i=N_{ele}}}{Nu_{evp,i=1}} \tag{13}$$

For the condensation process, Nusselt number is calculated using Yan's correlation (Yan *et al.*, 1999):

$$Nu = 4.118 \cdot Re_{eq}^{0.4} \cdot Pr_l^{0.33} \tag{14}$$

With the rated U_i and ΔT_i, the total heat transfer area A_{tot} can be given by:

$$A_{tot} = \sum_{i=1}^{N_{ele}} A_i \tag{15}$$

However, this calculated surface area must satisfy the input condition, i.e. the plate height of 2.31 m, which is achieved by varying the number of channels for each fluid until the objective error function (equation (16)) is minimized.

$$\Delta H(N_{ch}) = \frac{A_{tot}}{3 \cdot W} - H_{plate} \tag{16}$$

The total number of plates is thus given by:

$$N_{plate} = 3 \cdot (2 \cdot N_{ch} - 1) \tag{17}$$

5. Levelized Cost of Electricity

The economic performance of the considered geothermal ORC system is evaluated by means of the Levelized Cost of Electricity (LCOE) method. Based on the Net Present Value (NPV) method, LCOE is given by (Konstantin, 2013):

$$LCOE = \frac{I_0 + \sum_{t=1}^{t=n} \frac{A_t + I_t}{(1+r)^t}}{\sum_{t=1}^{t=n} \frac{W_{el}}{(1+r)^t}} \tag{18}$$

Where I_0 is the initial investment cost [€]; A_t is the expenditures for Operation & Maintenance (O&M) in the year t [€]; I_t is the investment costs for replacement of equipment in the year t [€]; W_{el} is the Electricity generation in the year t [MWh]; r is the annual discount rate [%]; n is the lifetime of the project in years [a].

Factors accounting for the initial investment cost I_0 are manifold, such as the costs for drilling, purchasing equipment, and other expenses such as site preparation, instrumentation, control, insurance, etc. For a drilling depth of 3.5 km, the drilling cost is estimated to about 21 Mio. € using the correlations from (Schlagermann, 2014). The Purchased Equipment Cost (PEC) related to the component parameters is described in detail see section 5.1. The other expenses for the initial investment are mainly dependent on the drilling process, which approximately accounts for 40% of the total drilling cost (Schlagermann, 2014).

Apart from the initial investment costs in equation (18), the annual expenditures for O&M are estimated to be about $0.03 \cdot I_0$ based on the proposed correlations (Schlagermann, 2014). The investment costs caused by the replacement of system components depend on the lifetime of each component (see table 3). The annual electricity generation is calculated with the consideration of 8000

full-load hours. The annual discount rate is set to 8%. Finally, the lifetime of the project is considered to be 25 years.

It is noted that the correlations used for the economic evaluation are based on an existing geothermal ORC plant in Germany. For more details, the reader is referred to Schlagermann (2014).

Table 3: Constants in equation (19), bare module factors and lifetimes for different system components (Turton *et al.*, 2013) (Schlagermann, 2014)

Equipment	K_1	K_2	K_3	F_B	Lifetime
Pump	3.3892	0.0536	0.1538	4.05	10
Preheater + Evaporator	4.6656	-0.1557	0.1547	3.86	10
Turbine	2.6259	1.4398	-0.1776	6.10	25
Condenser	4.6656	-0.1557	0.1547	3.86	10

5.1 Purchased Equipment Cost (PEC)

The PEC for each component of the ORC system is calculated using the empirical correlations based on a number of industrial data (Turton *et al.*, 2013), which is given by:

$$\log_{10} PEC_0 = K_1 + K_2 \cdot \log_{10} X + K_3 \cdot (\log_{10} X)^2 \tag{19}$$

Where K_1, K_2, K_3 are constants depending on the system component (see table 3) and X is the size or capacity for the corresponding component. The calculated PEC_0 is converted into Euro with the average exchange rate of 1.2 for the recent years.

The multiplication factor F_B is used to account for the indirect costs and the use of specific materials (Turton *et al.*, 2013). Therefore, the modified PEC is given by:

$$PEC = PEC_0 \cdot F_B \tag{20}$$

Where F_B is listed in table 3 for each of the system equipment.

The Chemical Engineering Plant Cost Index (CEPCI) is used to evaluate the cost deviation due to inflation. The PEC calculated using equation (20) is based on the CEPCI value of 382 for the year of 1996 (Turton *et al.*, 2013). In the present economic analysis, the updated value of 578.1 for the year of 2014 is employed.

6. Results

The main aim of the thermo-economic optimization is to obtain the minimum of LCOE for the considered two fluids, i.e. the selected R227ea and the reference fluid R245fa.

For R227ea with a constant evaporating pressure in the investigated ORC system, the influence of the pinch point (depicted in figure 3(a)) on the ORC system performance is threefold. Firstly, according to equation (4), increasing the pinch point temperature results in a higher OHST value, which can change the pinch point position to the evaporator inlet in the case of OHST > T$_{hs}$. In order to avoid such changes, the pinch point value is limited up to 15 K for which the OHST is equal to 139.93 °C. Secondly, increasing the pinch point temperature corresponds to a worse thermal match between the thermal water and the working fluid, which reduces the system efficiency. Such influence is illustrated in figure 5 where the global system efficiency for R227ea decreases monotonically with the increase of the pinch point value. Thirdly, the benefit of increasing the pinch point is that it requires a smaller heat transfer area, leading to a lower PEC value particularly for the preheater and the evaporator. Particularly for R227ea, it can be seen from figure 5 that the total PEC for the preheater and the evaporator decreases significantly with the increase of the pinch point value. A small decrease in the other costs mainly referring to the instrumentation & controlling is also observed for a higher pinch point value. The PEC for condenser, turbine and pump are relatively less affected by varying the pinch point. Conclusively, it is reasonable to consider the pinch point in the heat exchanger as the optimization parameter for R227ea.

It is necessary to note that due to the consideration of the constant condensation temperature the variation of the pinch point for the condenser affects only the condenser size but not the power output. Therefore, its influence on the LCOE is relatively limited so that it is not considered in the present techno-economic optimization.
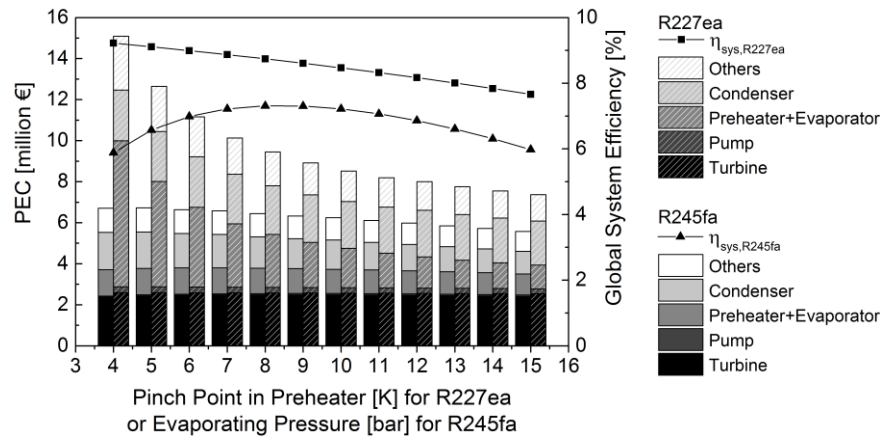
Figure 5: PEC and system efficiency as functions of $\Delta T_{pp,evp}$ and p_{evp} for R227ea and R245fa, respectively.
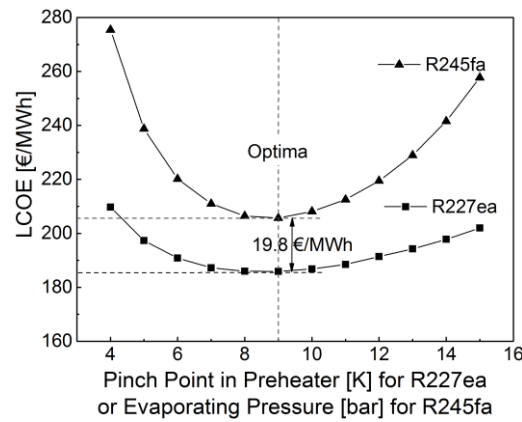

Figure 6: LCOE as functions of $\Delta T_{pp,evp}$ and p_{evp} for R227ea and R245fa, respectively.

Figure 6 shows the resulting LCOE with the variation of pinch point. For R227ea, the minimum of LCOE is observed around 185.9 €/MWh for the pinch point of 9 K. In order for such minimum to make sense, it is required to compare it to the optimum LCOE for some other fluid, e.g. the reference fluid R245fa. The optimization parameter for R245fa, however, is different from that for R227ea. According to equation (4), the OHST for R245fa is significantly higher than the available heat source temperature, indicating that the pinch point is located at the evaporator inlet (see figure 3(b)). In such case to obtain the minimum LCOE, the evaporating pressure is chosen as the optimization parameter (Quoilin *et al*., 2011). In contrast to R227ea, the pinch point in the preheater is fixed at 4 K for R245fa. In figure 5, the PEC and global system efficiency for R245fa are shown as a function of evaporating pressure, where a maximum global system efficiency can be observed. The LCOE for R245fa is given in figure 6 as a function of evaporating pressure, where a minimum is observed for the evaporating pressure of 9 bar.

For further comparisons, the T-Q diagrams for the optimized R227ea and R245fa are given, illustrating their heat transfer processes, respectively. In addition, table 4 summarizes the parameters resulting from the thermo-economic optimizations for both working fluids. Although the use of R227ea requires higher PEC, more electricity can be produced annually, which leads to reduce the LCOE by 9.63%.

Table 4: Results from the thermo-economic optimizations for R227ea and R245fa

Fluid	Thermodynamic						Economic	
	T_{evp} [°C]	p_{evp} [bar]	$T_{pp,evp}$ [K]	η_{sys} [%]	η_{HT} [%]	W_{el} [MWh]	PEC [m. €]	$LCOE$ [€/MWh]
R227ea	96.60	26.33	9.000	8.607	79.47	29006	8.739	185.9
R245fa	85.33	9	4.000	7.306	63.51	23762	7.306	205.7

7. Conclusions

In the present paper, a new approach for the heat transfer optimization has been developed and thermo-economically investigated for a sub-critical ORC designed for geothermal power generation. The working fluid considered is R227ea, for which the pinch point is not located at the evaporator inlet for the available heat source temperature. A detailed heat transfer model is proposed, aiming at the precise determination of the pinch point position and the calculation of the required heat transfer area. Compared to common works, the optimization parameter considered for R227ea is not the evaporating pressure but the pinch point for the heat transfer process. The results show that the pinch point in the preheater has a great influence on both of the system efficiency and the PEC. An optimum pinch point value is obtained for R227ea, corresponding to a global system efficiency of 8.607% and a minimum LCOE of 185.9 €/MWh. Compared to the optimization results for R245fa, an increase of system efficiency of 17.81% and a reduction of LCOE of 9.63% are observed.

In general, the proposed approach leading to both higher system efficiency and economic profitability seems promising. However, further challenges remain. The numerical results should be compared with the experimental results in the near future. In addition, it is necessary to further include pressure drops through the ORC loops and to investigate their influences on the heat transfer mechanism particularly for the working fluid at the near-critical states.

NOMENCLATURE

A	Surface area or annual cost	(m^2 or €)
b	Channel space	(mm)
c_p	Specific heat capacity	(kJ/kg·K)
d	Plate thickness	(mm)
D_h	Hydraulic diameter	(m)
e	Specific exergy flow	(kJ/kg)
F_B	Multiplication factor for PEC	(-)
h	Specific enthalpy	(kJ/kg)
h	Convective heat transfer	(W/kg·m^2)
H	Plate height	(m)
I	Investment cost	(€)
K	Constants for PEC	(-)
m.	million	(€)
$\dot{m}$	Mass flow rate	(kg/s)
n	Lifetime of project	(a)
Nu	Nusselt number	(-)
p	Pressure	(bar)
P	Power	(kW or MW)
Pr	Prandtl number	(-)
$\dot{Q}$	Heat flow	(kW)
r	Annual discount rate	(%)
Re	Reynold number	(-)
t	Operation year	(-)
T	Temperature	(°C)
U	Overall heat transfer coeff.	(W/kg·m^2)
W	Plate width	(m)
W	Electricity generation	(MW)
x	Vapor fraction	(-)
X	Size or capacity	(m^2 or kW)
β	Corrugation angle	(°)
η	Efficiency	(%)
λ	Thermal conductivity	(W/m·K)

μ	Viscosity	(kg/s·m)
ρ	Density	(kg/m^3)

Subscript

0,1,2,...10	Reference or working states		pre	Preheater
el	Electricity		sys	System
ele	Element		th	Thermal
eq	Equivalent		tot	Total
evp	Evaporation		v	Saturated vapor
G	Generator		wf	Working fluid
hs	Heat source		**Acronyms**	
HT	Heat transferred		$LCOE$	Levelized Cost of Electricity
l	Saturated liquid		ORC	Organic Rankine Cycle
$mech$	Mechanical		$OHST$	Optimal Heat source temperature
M	Motor		PEC	Purchased Equipment Cost
pp	Pinch point		PHE	Plate Heat Exchanger

REFERENCES

Chisholm, D., Wanniarachchi, A.S., Plate heat exchangers: plate selection and arrangement, *AIChE Meeting*, 18-22.

Heberle,F., Preißinger,M., Brüggemann, D, 2012, Zeotropic mixtures as working fluids in Organic Rankine Cycles for low-enthalpy geothermal resources, *Renewable Energy,* vol. 37, no. 1, p. 364–370.

Karellas, S., Schuster,A., Leontaritis, A., 2012, Influence of supercritical ORC parameters on plate heat exchanger design, *Applied Thermal Engineering,* vol. 33-34, p. 70–76.

Khennich, M., Galanis, N., 2012, Optimal Design of ORC Systems with a Low-Temperature Heat Source, *Entropy,* vol. 14, no. 12, p. 370–389.

Konstantin, P., 2013, *Praxisbuch Energiewirtschaft. Energieumwandlung, -transport und -beschaffung im liberalisierten Markt,* Springer Vieweg , Berlin, 474.

Lemmon E.W., Huber, M.L., Nist reference fluid thermodynamic and transport properties-refprop, NIST standard reference database 23-Version 9.0.

Liu, W., Meinel, D., Wieland, C., Spliethoff, H., 2014: Investigation of hydrofluoroolefins as potential working fluids in organic Rankine cycle for geothermal power generation, *Energy,* vol. 67, p. 106-116.

Liu, W., Meinel, D., Wieland, C., Spliethoff, H., 2015: Optimal Heat Source Temperature for Optimization of the Organic Rankine Cycle (ORC) process. Submitted In *Energy* 2015.

Quoilin, S., Declaye, S,. Tchanche, B.F., Lemort, V., 2011, Thermo-economic optimization of waste heat recovery Organic Rankine Cycles, *Applied Thermal Engineering,* vol. 31, p. 2885–2893.

Schlagermann, P., 2014, *Exergoökonomische Analyse geothermischer Strombereitstellung am Beispiel des Oberrheingrabens,* Dr. Hut, Munich, 168.

Schuster, A., Karellas, S., Aumann, R., 2010, Efficiency optimization potential in supercritical Organic Rankine Cycles, *Energy,* vol. 35, no. 2, p. 1033–1039.

Turton, R., Bailie, R.C., Whiting, W.B., Shaeiwitz, J.A., Bhattacharyya, D., 2013, *Analysis, Synthesis, and Design of Chemical Processes*, Pearson, NY, 965.

Yan, Y.Y., Lin, T. F., 1999, Evaporation Heat Transfer and Pressure Drop of Refrigerant R-134a in a Plate Heat Exchanger, *Journal of Heat Transfer,* vol. 121, p. 118–127.

Yan, Y.Y., Lio, H.C., Lin, T.F., 1999, Condensation heat transfer and pressure drop of refrigerant R-134a in a plate heat exchanger, *International Journal of Heat and Mass Transfer,* vol. 42, no. 6, p. 993–1006.